Article Identifier
DOI: 10.22032/dbt.58841
URN: urn:nbn:de:gbv:ilm1-2023isc-079:2

60th ILMENAU SCIENTIFIC COLLOQUIUM Technische Universität Ilmenau, 4 – 8 September 2023
URN: urn:nbn:de:gbv:ilm1-2023isc:1

VALIDATION OF EXPERIMENTAL SETUP FOR AEROSTATIC BEARING SIMULATION

Mikael Miettinen[1], Valtteri Vainio[1], Petteri Haverinen[1], Onni Leutonen[1], Raine Viitala[1], René Theska[2]

[1] Mechatronics Group, Aalto University, Espoo, Finland
[2] Precision Engineering Group, TU Ilmenau, Germany

ABSTRACT

Aerostatic bearings are extensively used in precision engineering applications that require high positional accuracy and low friction motion. In these bearings, externally pressurized gas is fed through a restrictor into the bearing gap. The viscous shear in the gap restricts the flow, thus forming a pressurized film between the bearing and the guide surface.

In the development of models and in investigations of, for example, effects of manufacturing errors and porous material permeability properties, characterization of bearing performance is required. The performance is commonly characterized with a measurement setup, either under static or dynamic conditions. In the present study, an experimental setup for the measurement performance of aerostatic bearings is presented. The investigated measurement setup is validated with a comparison to a literature model.

The results of the present study include the load capacity, stiffness, air consumption, and pressure distribution of a commercially available axisymmetric graphite thrust bearing. The results show good agreement between the measurements and the model. Thus, the results show corroborative evidence on the usability of the measurement setup in future aerostatic bearing research.

Index Terms - Aerostatic bearing, porous restrictor

1. INTRODUCTION

Aerostatic bearings are commonly used in precision motion applications requiring high positioning accuracy. The main contributing factors to the widespread utilization in precision engineering solutions include the low friction and inherently small error motions due to the gas film averaging short wavelength errors in the guide surface. Aerostatic bearings are commonly either compensated with orifice or porous restrictors. The present study focuses on aerostatic bearings with porous restrictors. Aerostatic bearings have been extensively studied, both with experimental and theoretical investigations on their static and dynamic behavior [1,2].

In experimental research, there are numerous test setups for the measurement of the performance of air bearings. Commonly, the experimental setups consist of a load frame to load the bearing against its guide surface, and a measurement frame to measure the gap height and other quantities of interest. The measurement setups for aerostatic thrust bearings commonly

© 2023 by the authors. – Licensee Technische Universität Ilmenau, Deutschland.
This is an Open Access article distributed under the terms of the Creative Commons Attribution ShareAlike-4.0 International License, (https://creativecommons.org/licenses/by-sa/4.0/).

load the bearing by means of a mass [3-5], a screw [6,7], a pneumatic actuator [8], or a hydraulic actuator [9] in the static performance characterization setups. In investigations of response to dynamic loading, a piezoelectric actuator [10] or a voice coil [11-13], or even a hit of an impulse hammer [14] can be used either individually or in combination with one of the methods of the static setups. The pressure in the gap between the bearing and the guide surface has been measured with, for example, pressure sensors embedded in the guide surface or the bearing [8,9,15], pressure-sensitive films [16], or paints [17]. The height of the air gap is commonly measured with displacement sensors that measure the relative displacement of the bearing with the air supply on and off [5,8,10,13,17].

For the development of simulation models, measurement setups that produce accurate performance data are required for the validation of the models. Furthermore, the setups are useful in the investigation of influences on the behavior of the bearing, such as the effects of manufacturing errors and material properties of the restrictor. Despite the rigorous efforts in the research of aerostatic bearings, further development of models, materials, and designs are still matters of ongoing scientific activities.

Therefore, the present study experimentally validates a measurement setup for static measurement of aerostatic bearing performance. A preliminary study of the investigated setup has been previously published [8]. However, in the present study, the uncertainty of the air gap measurements was significantly reduced with improvements to the structure of the setup and the utilization of higher accuracy sensors for the gap height measurement. The investigated measurands are the load capacity, static stiffness, air consumption, and the radial pressure distribution in the air gap. The validation is performed by comparing the measurement results to a verified literature model, published by Plante et al. [18].

2. METHODS

2.1. Investigated bearing

The investigated bearing was an axisymmetric porous aerostatic thrust bearing, model S104001 from New Way Air Bearings (Figure 1). The bearing consists of a graphite restrictor with a diameter of 36.83 mm and an aluminum body. The restrictor is adhesively bonded to the body of the bearing. The body of the bearing features a ball socket, from which the bearing can be mounted onto a stud with a ball tip of a matching radius.

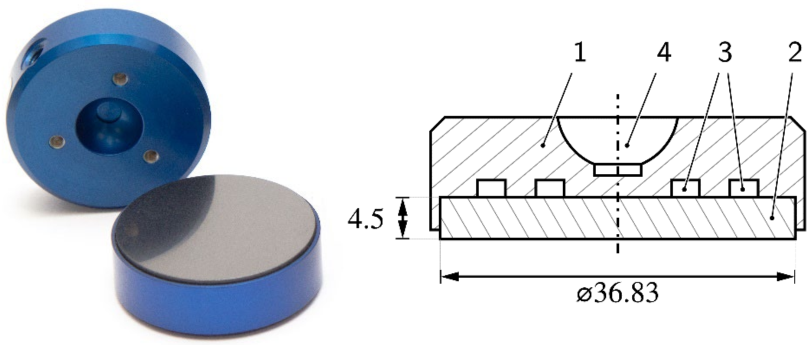

Figure 1. Investigated porous aerostatic bearing and the dimensions of the restrictor. Main components and features annotated in the cross-sectional drawing: 1 Body, 2 Porous restrictor, 3 Air supply grooves, 4 Ball socket.

© 2023 by the authors. – Licensee Technische Universität Ilmenau, Deutschland.

2.2. Experimental setup

The investigated measurement setup consists of a loading mechanism to load the investigated thrust bearing against a guide surface, and sensors to measure the load, the gap height, the air flow, and the pressure distribution in the air gap of the bearing. A kinematic representation of the measurement setup is presented in Figure 2. The bearing was supported with a parallel spring flexure mechanism, which constrains the motion of the bearing to only the vertical direction. The bearing was connected to the flexure mechanism with a ball-socket joint, allowing the bearing to orient itself parallel to the guide surface. The bearing was loaded against the guide surface with a low friction pneumatic actuator. The guide surface was movable, allowing the measurement of the radial pressure distribution of the air gap with a pressure sensor embedded into the guide. The motion of the guide was implemented with a monolithic parallel spring guide mechanism, with two pairs of springs in series to limit the parasitic displacement. The motion was actuated with a stepper motor and a lead screw.

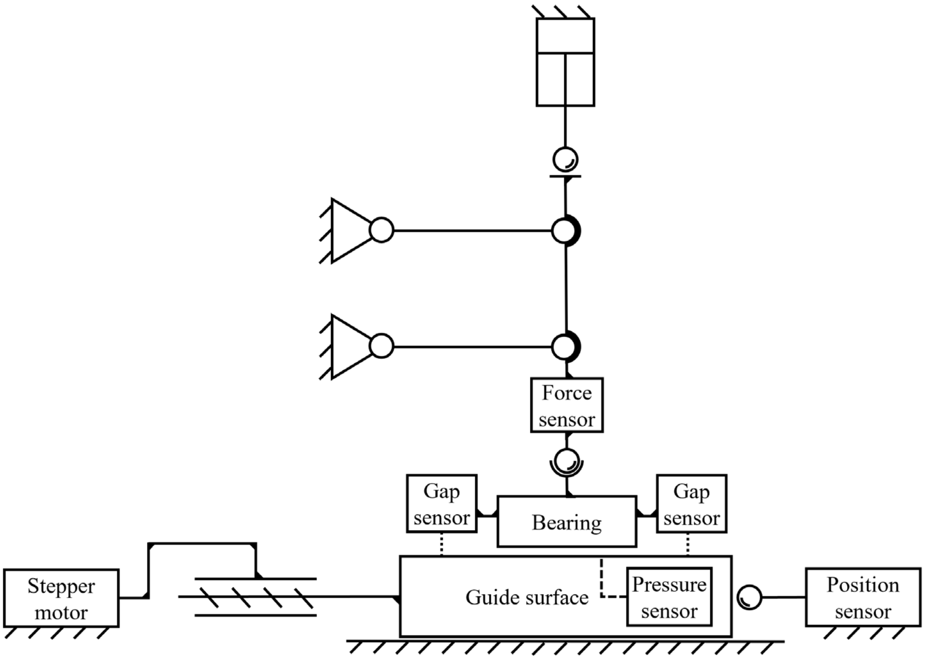

Figure 2. Kinematic model of the measurement setup. A parallel spring flexure is used to constrain the bearing to pure vertical motion. The bearing is oriented parallel to the guide surface with a spherical joint. The bearing is loaded against the guide surface with a low-friction pneumatic actuator.

The setup is presented in Figure 3. The structural loop of the loading mechanism was separated from the structural loop of the measurement system in order to reduce uncertainties, especially in the gap height measurement. The measurement loop consisted of the investigated bearing, the guide surface, and the gap height sensors, and the sensor holder. Of which only the investigated bearing and the guide surface were part of the load path. The guide surface was a steel plate that was resting on top of the natural stone cube, i.e., there was a plane-plane contact between the guide and the cube. The high surface area of the contact improves the stiffness of the joint. However, care was needed to be taken in order to limit any potential adverse effects due to overconstrainment. The surface of the cube was ground to the flatness of less than 1 µm, as was the top and the bottom of the guide. In addition, grinding of the guide surface top and bottom surface to the flatness and parallelism was conducted after the machining of the flexure mechanism. Further, the intermediate bodies of the parallel spring guide were relieved to not touch the surface of the cube. With these mitigating actions, and the separation of the metrology loop from the motion mechanism a well-behaving system was achieved.

© 2023 by the authors. – Licensee Technische Universität Ilmenau, Deutschland.

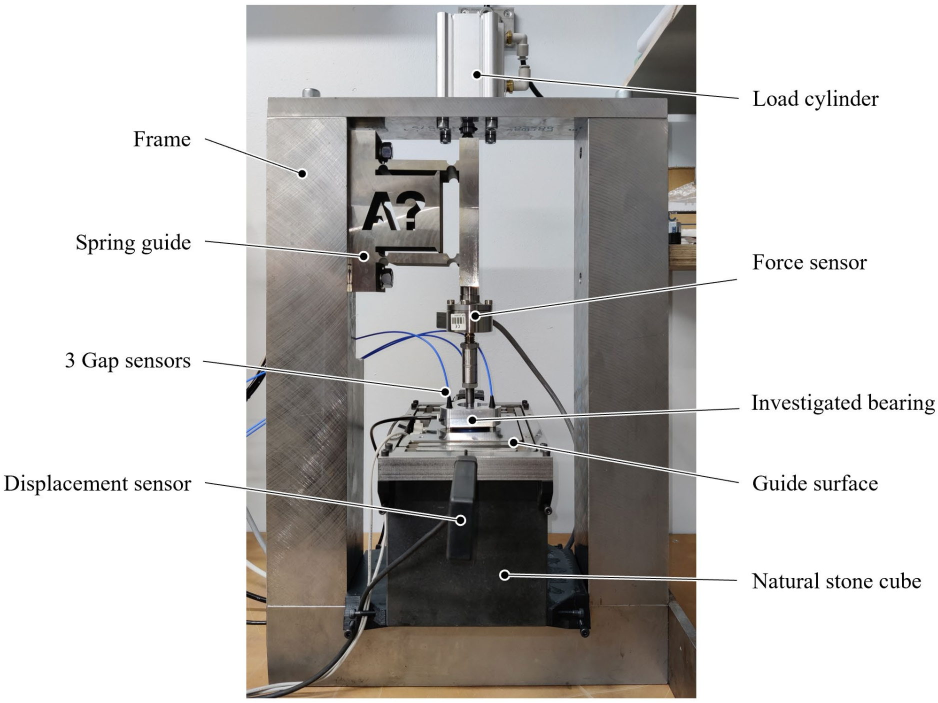

Figure 3. Measurement setup.

The load on the bearing was measured with a force sensor located between the flexure mechanism and the bearing. The bearing supply pressure and air flow into the bearing were measured at the supply line. The air gap pressure distribution measurement was more elaborate. The air gap pressure was measured with a pressure sensor embedded in the guide surface. A 0.1 mm hole located in the top surface of the guide connected the air gap to the sensor. As the guide surface was movable, the pressure measurement hole could be moved stepwise to any radial position under the bearing. Finally, the position of the movable guide was measured with a Heidenhain mt-25 displacement sensor and EIB 742 interface electronics.

The measurement data was recorded with a NI-cDAQ-9185 chassis with NI 9205 analog input module and NI9237 bridge module. NI 0262 analog output module was used to control pressure regulators. In addition, a Micro-Epsilon DT6220 controller with DL6220 demodulators was used for the capacitive gap height measurement sensors. A list of the sensors and their accuracies is presented in Table 1.

Table 1. Sensors used in the measurement setup.

Device	**Type**	**Range**	**Accuracy**
Pressure regulator	SMC ITV1050	0 – 0.6 MPa	±2% FS
Pressure sensor	SMC PSE540A	0 – 0.6 MPa	±1% FS
Flow sensor	SMC PF2M725	0 – 5 L/min	±5% FS
Air gap height sensor	Micro-Epsilon CSH-05	0 – 500 µm	±0.3% FS
Load sensor	HBM U2B	0 – 1 kN	
Guide surface displacement sensor	Heidenhain MT-25	0 – 25 mm	

© 2023 by the authors. – Licensee Technische Universität Ilmenau, Deutschland.

2.2. Validation model

The measurements were validated against a model published by Plante et al. [18]. The model is a 1D model of the air gap. In his work, the porous restrictor is modeled with Darcy's Law, and the air gap is modeled with Mach equations and is solved iteratively. In the original publication, the model was verified with experimental measurements [18].

The permeability of the porous restrictor is an essential prerequisite for modeling the flow through the restrictor. The permeability can be determined experimentally by measuring the short circuit flow, i.e., the flow with no gap restriction. Thus, the permeability of the porous restrictor k is [5,19]:

$$k = \frac{Q\mu H p_a}{A(p_s^2 - {p_a}^2)}$$

Where Q is the short circuit flow of the bearing, p_s is the supply pressure, p_a is the ambient pressure, A is the area of the restrictor, μ is the dynamic viscosity of air and H is the height of the porous restrictor. This method is based on the linear Darcy's law. The measured short circuit flow through the porous restrictor was 2.69 L/min at 0.6 MPa supply pressure. Thus, the permeability of the porous restrictor was 1.44e-15 m^2.

3. RESULTS

The results of the measurements are presented in comparison to the results of the model of Plante et al [18]. Three supply pressures, 0.2 MPa, 0.4 MPa, and 0.6 MPa were tested. For the simulations, air gap heights of 1 to 19 µm at 1 µm increments are shown. For the measurements, loads from 25 N to 500 N with 25 N increments were used. Measurement points with a gap height in the range of 1 to 19 µm are shown. The load capacity of the bearing is presented in Figure 4, the static stiffness of the bearing is presented in Figure 5, and the air flow through the bearing is presented in Figure 6.

The air gap pressure profile is presented in Figure 7. Since the simulation results refer to a gap height of 4 µm, the measurement results closest to the gap height of 4 µm are used for comparison. The pressure shown is relative pressure.

In addition to the measurements of bearing performance, the deformation of the metrology loop of the setup is presented (Figure 8). The displacement measured by the air gap height sensors is shown with 0 MPa supply pressure to the bearing.

© 2023 by the authors. – Licensee Technische Universität Ilmenau, Deutschland.

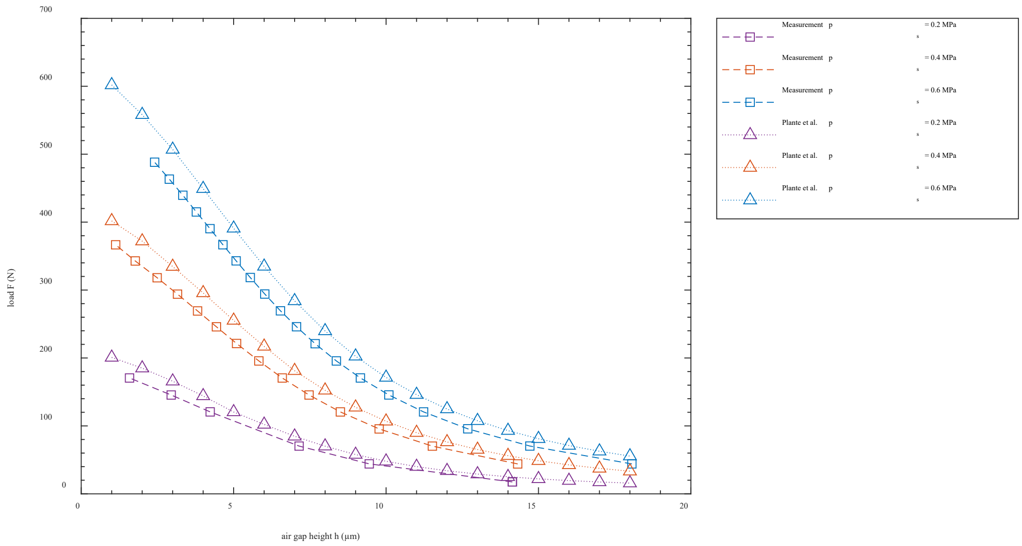

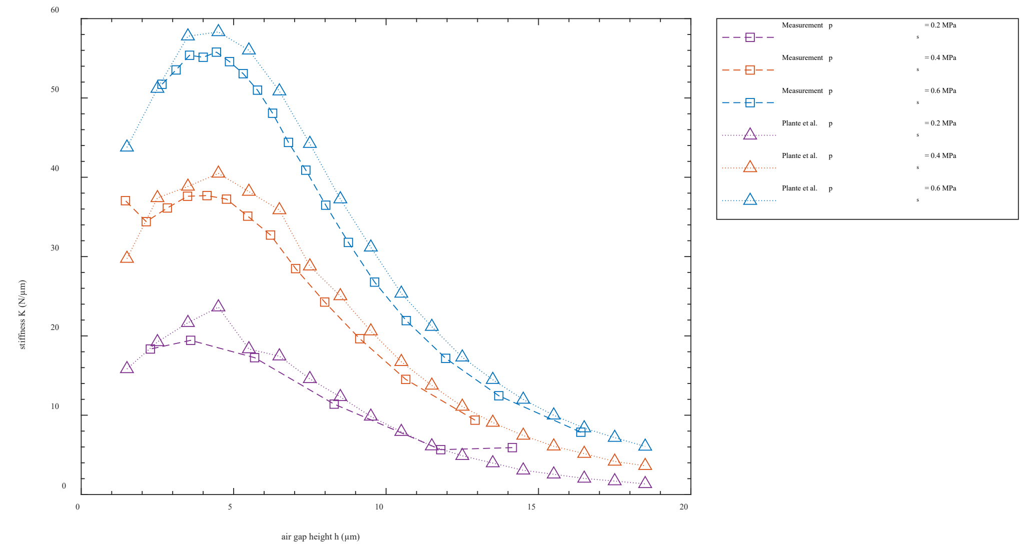

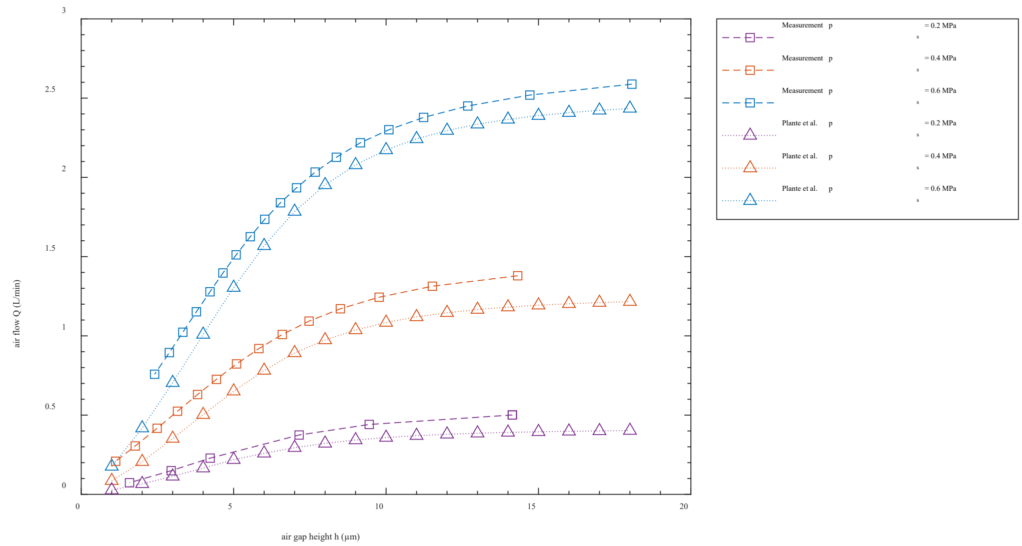

© 2023 by the authors. – Licensee Technische Universität Ilmenau, Deutschland.

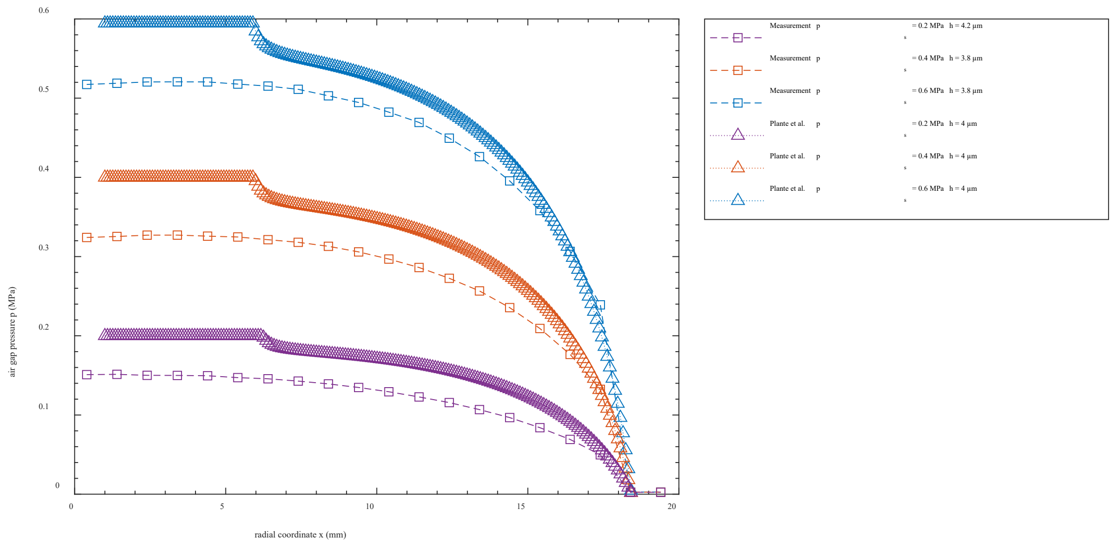

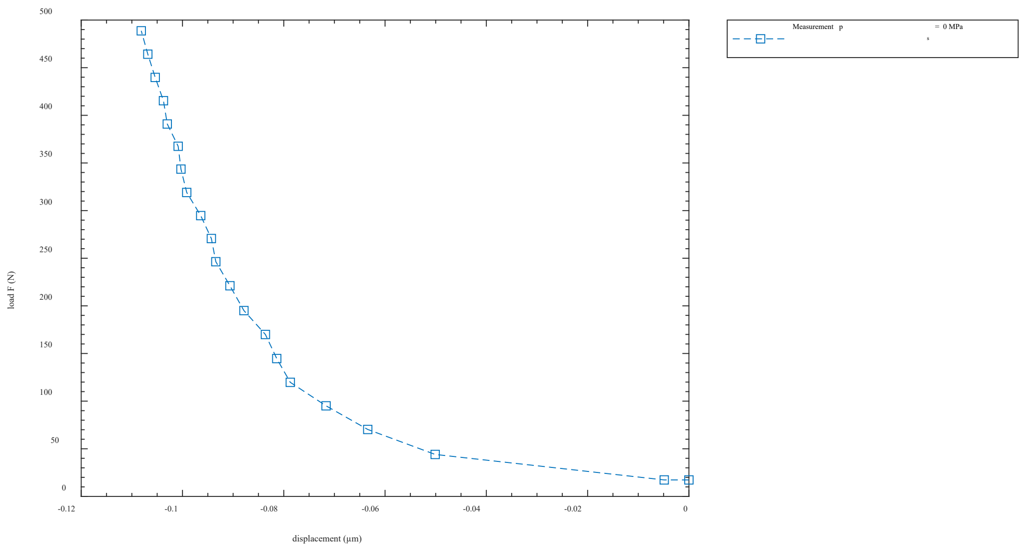

4. DISCUSSION

In the present study, there is an apparent broad qualitative agreement between the experimental results and those obtained from the simulation model of Plante et al [18]. The measured load capacity, and thus the stiffness is slightly lower than the model estimation. In contrast, the measured air flow is slightly larger than the model. However, the differences between the results of the measurement and the model are small.

In the simulation model, the gap height is given as an input and the load is obtained as a result. In contrast, the opposite is true for the measurement setup. The load is set as an input to the actuator, and the actual load and the gap height are obtained as results. Thus, there is a small

© 2023 by the authors. – Licensee Technische Universität Ilmenau, Deutschland.

discrepancy in the gap heights in Figure 7. This has a small effect on the pressures, as the pressure in the gap is higher at lower gap heights.

Furthermore, alignment of the radial position of the measured pressure distribution to the simulation data leads to some uncertainty in the radial position. The motion range of the movable guide surface is only measured relatively. Thus, the measurement data has to be aligned by placing the point where the measured gap pressure drops to the ambient pressure at the outer radius of the bearing.

The pressure distribution of the model by Plante et al. has a characteristic shape due to the modelling method (Figure 7). The constant pressure region and the following rapid change originates from the methods used to overcome a singularity in the Mach equations at zero flow velocity. This singularity has been avoided in the model by introducing a constant pressure region to the center area and iterating the pressure level and the radius of the area until the model converges to a solution. Thus, the results of the model do not accurately depict the shape of the distribution.

The influence of the loading on the air gap height metrology loop was verified by measuring the deformation of the metrology loop with the air gap sensor with 0 MPa supply pressure (Figure 8). Thus, the behavior of the setup could be characterized. The results show that the deformation is small, thus a separation between the load loop and measurement loop was achieved. Further, the measured deformation can be used as compensation for the air gap height measurements.

The present study omits detailed uncertainty analysis for brevity. However, care was taken to limit the effects of potential error sources. The measurements were made in a temperature-controlled room, dry and clean air was used to supply the bearing and the setup was designed separate the gap height measurement loop from the structural loop of the setup. Taking to account the low deformation of the measurement setup (Figure 8) and accuracies of the used sensors in (Table 1), the results of the present study are deemed valid.

5. CONCLUSION

In the present study, a static measurement setup for static performance characterization of aerostatic bearings was proposed. The setup was validated with a comparison to a simulation model. Measurements of load capacity, static stiffness, air flow and radial pressure distribution of a commercially available bearing were compared. Additionally, the deformation of the measurement loop while the bearing was loaded was investigated.

The present study shows that the results obtained with the measurement setup are in good agreement to the literature model and behave in accordance with the known behavior of aerostatic bearings in the current body of knowledge. Therefore, the measurement setup was found to be valuable for studying the static performance of air bearings. In future work, the measurement setup will be used for investigating the effects of restrictor material permeability properties and manufacturing errors on bearing performance. In addition, the setup will be used to test further optimized simulation models that are currently being researched.

© 2023 by the authors. – Licensee Technische Universität Ilmenau, Deutschland.

REFERENCES

[1] Q. Gao, W. Chen, L. Lu, D. Huo, and K. Cheng, "Aerostatic bearings design and analysis with the application to precision engineering: State-of-the-art and future perspectives," *Tribol. Int.*, vol. 135, pp. 1–17, 2019, doi: 10.1016/j.triboint.2019.02.020.

[2] T. Raparelli, V. Viktorov, F. Colombo, and L. Lentini, "Aerostatic thrust bearings active compensation: Critical review," *Precis. Eng.*, vol. 44, pp. 1–12, Apr. 2016, doi: 10.1016/J.PRECISIONENG.2015.11.002.

[3] H. S. Chang, Z. S. Wang, and D. C. Sun, "An Experimental Investigation of the Stability of Externally Pressurized Gas-Lubricated Porous Thrust Bearings," *J. Lubr. Technol.*, vol. 105, no. 4, pp. 630–637, Oct. 1983, doi: 10.1115/1.3254695.

[4] P. Wang *et al.*, "Study on the pneumatic hammer phenomenon of aerostatic bearings based on the empirical mode method: Numerical and experimental analysis," *Tribol. Int.*, vol. 181, Mar. 2023, doi: 10.1016/j.triboint.2023.108305.

[5] M. Hübner, M. Miettinen, V. Vainio, C. Cierpka, R. Theska, and R. Viitala, "Behaviour of porous aerostatic bearings with various restrictor permeabilities," in *Proceedings of the 21st International Conference of the European Society for Precision Engineering and Nanotechnology, EUSPEN 2021*, 2021, no. June, pp. 115–118.

[6] C. Schenk, "Theoretische und experimentelle Untersuchungen an ebenen aerostatischen Gaslagerelementen unter Hochvakuumbedingungen," Technische Universität Ilmenau, 2007.

[7] N. Heidler, "Untersuchungen zylindrischer Gasführungselemente für Hochvakuumanwendungen," Technische Universität Ilmenau, 2015.

[8] V. Vainio, J. Majuri, M. Miettinen, and R. Viitala, "Air gap pressure distribution measurement device," in *Proceedings of the 23rd international conference of the european society for precision engineering and nanotechnology*, 2023, pp. 249–250.

[9] N. Bhat, S. Kumar, W. Tan, R. Narasimhan, and T. C. Low, "Performance of inherently compensated flat pad aerostatic bearings subject to dynamic perturbation forces," *Precis. Eng.*, vol. 36, no. 3, pp. 399–407, Jul. 2012, doi: 10.1016/j.precisioneng.2012.01.002.

[10] N. Maamari, "Smart Active Aerostatic Bearing," ETH Zurich, 2019.

[11] P. Holster, J. Jacobs, and J. Roblee, "The Measurement and Finite Element Analysis of the Dynamic Stiffness of Nonuniform Clearance, Gas, Thrust Bearings," *J. Tribol.*, vol. 113, no. 4, pp. 768–774, Oct. 1991, doi: 10.1115/1.2920691.

[12] P. Plessers and R. Snoeys, "Dynamic Identification of Convergent Externally Pressurized Gas-Bearing Gaps," *J. Tribol.*, vol. 110, no. 2, pp. 263–270, Apr. 1988, doi: 10.1115/1.3261597.

[13] F. Colombo, L. Lentini, T. Raparelli, A. Trivella, and V. Viktorov, "Dynamic Characterisation of Rectangular Aerostatic Pads with Multiple Inherent Orifices," *Tribol. Lett.*, vol. 66, no. 4, p. 133, Dec. 2018, doi: 10.1007/s11249-018-1087-x.

[14] R. H. M. Franssen, W. Potze, P. de Jong, R. H. B. Fey, and H. Nijmeijer, "Large amplitude dynamic behavior of thrust air bearings: Modeling and experiments," *Tribol. Int.*, vol. 109, pp. 460–466, May 2017, doi: 10.1016/j.triboint.2016.12.024.

[15] W. Li, S. Wang, and K. Feng, "Numerical and experimental study on the effect of surface damages on the performances of porous aerostatic bearings," *Tribol. Int.*, vol. 175, p. 107791, Nov. 2022, doi: 10.1016/j.triboint.2022.107791.

[16] Y. Zhou, X. Chen, Y. Cai, H. Chen, and B. Han, "Measurement of gas pressure distribution in aerostatic thrust bearings using pressure-sensitive film," *Tribol. Int.*, vol. 120, pp. 9–15, Apr. 2018, doi: 10.1016/j.triboint.2017.12.002.

© 2023 by the authors. – Licensee Technische Universität Ilmenau, Deutschland.

[17] A. L. Zimmermann, R. H. M. Giepman, Q. T. Nguyen Tran, C. Aalburg, and V. Gümmer, "Design of a static test rig for advanced seals and air bearing testing," in *Open Archives of the 17th International Symposium on Transport Phenomena and Dynamics of Rotating Machinery, ISROMAC 2017*, 2017, no. January 2018.
[18] J. S. Plante, J. Vogan, T. El-Aguizy, and A. H. Slocum, "A design model for circular porous air bearings using the 1D generalized flow method," *Precis. Eng.*, vol. 29, no. 3, pp. 336–346, Jul. 2005, doi: 10.1016/j.precisioneng.2004.11.011
[19] W. H. Rasnick, T. A. Arehart, D. E. Littleton, and P. J. Steger, "Porous graphite air-bearing components as applied to machine tools," Dearborn, 1974.

CONTACT

Mikael Miettinen email: mikael.miettinen@aalto.fi
ORCID: https://orcid.org/0000-0002-9722-6756

Valtteri Vainio email: valtteri.s.vainio@aalto.fi

Petteri Haverinen email: petteri.haverinen@aalto.fi

Onni Leutonen email: onni.leutonen@aalto.fi

Prof. Raine Viitala email: raine.viitala@aalto.fi
ORCID: https://orcid.org/0000-0003-1672-1921

Prof. René Theska email: rene.theska@tu-ilmenau.de
ORCID: https://orcid.org/0000-0003-0589-8270

© 2023 by the authors. – Licensee Technische Universität Ilmenau, Deutschland.